Inorganica Chimica Acta, 20 (1976) 221–229

Adducts of Tin(IV) Tetrahalides with Neutral Lewis Bases. I. Vibrational Study of the *Cis–Trans* Isomerism in Solution*

S. J. RUZICKA and A. E. MERBACH

Institut de chimie minérale et analytique, Université de Lausanne, CH-1005 Lausanne, Switzerland

Received May 15, 1976

A large number of $SnX_4 \cdot 2L$ and $SnX_4 \cdot L{-}L$ tin(IV) tetrahalide adducts were synthesized and analyzed (X = Cl, Br; L = Me_2O, Et_2O, THF, Me_2S, Et_2S, THT, Me_2Se, MeCN, Me_3CCN, Me_2CO, HMPA, TMPA; L–L = $(MeOCH_2-)_2$). Their cis or trans geometry was determined by infrared and Raman spectroscopy. For the $SnCl_4 \cdot 2THT$ adduct, both isomers could be isolated by changing the solvent polarity. The existence of a cis–trans equilibrium in solution has been demonstrated for the majority of the adducts by Raman measurements. This equilibrium strongly depends upon the solvent polarity, the cis *isomer being favoured in a highly polar medium. Using a simplified model for Wilson's F–G matrices, the Sn–X force constants were determined and the following sequences deduced for the strength of the tin–ligand bond in $SnX_4 \cdot 2L$: $Me_2Se > Me_2S \sim THT \sim Et_2S > Me_2O \sim THF \sim Et_2O$ and HMPA > TMPA.*

Introduction

In the last ten years, a large number of studies have been devoted to the chemistry of tin(IV) tetrahalide adducts. The Lewis acid character of tin tetrahalides is demonstrated by their ability to form 1:1 and 1:2 adducts with unidentate bases; the latter adducts, $SnCl_4 \cdot 2L$, may exist as *cis* or *trans* isomers. Dumas and Gomel [1] have recently reviewed the studies concerning these compounds. Compared to the amount of measurements, the conclusions look poor; the high hygroscopy of tin tetrahalides and inadequate choice or use of analytical techniques led to conflicting results; the structure determination by means of vibrational spectroscopy often led to erroneous assignments when both techniques (infrared and Raman) were not used simultaneously. These different factors as well as nearly no solution measurements led to contradictory conclusions about the factors governing the *cis* or *trans* isomer formation, as well as the nature of the acid base interaction. We decided to undertake a systematic study on 1:2 tin tetrahalide adducts. In this paper, we shall determine their structure in the solid state and examine their behaviour in solution. We have synthesized a series of new complexes and some compounds already reported in the litterature in order to confirm or complete the proposed vibrational assignments.

*Abstracted, in part, from the Ph.D. thesis No 237 of S. J. Ruzicka, Swiss Federal Institute of Technology, Lausanne, 1976.

Experimental

All manipulations were carried out in a drybox (Kewaunee Scientific Equipment 2C2411). The humidity, measured with a Dupont 26-303 Moisture Analyser, is about 6 ppm of water.

Chemicals

Tin tetrahalides were distilled under vacuum. Dialkyloxides and sulfides, phosphorylated ligands, nitriles, acetone and solvents were dried and purified by standard methods. Dimethylselenium (Strem Chem.) was used without further purification.

$SnX_4 \cdot 2L$

A 10% excess of a 10% solution of the ligand in CH_2Cl_2 was added to a 10% solution of the tin tetrahalide in CH_2Cl_2 (n-pentane for *cis*-$SnCl_4 \cdot 2THT$). The adduct solution was then evaporated to dryness under nitrogen; the solid adduct was crushed and dried under 5×10^{-2} torr for 15 minutes. For $SnCl_4 \cdot 2TMPA$, a deliquescent solid was obtained after the first evaporation: the product was left 24 hours at −15 °C and dried for one hour at 5×10^{-2} torr. The vibrational spectra were recorded immediately after synthesis. The elemental analyses were performed by A. Bernhardt, 5251-Elbach, Germany, and are presented in Table I.

Solutions of $SnX_4 \cdot 2L$

The solutions were prepared by adding to a 10% tin tetrahalide solution an excess of a 10% ligand solution, in a 1:4 Sn/L ratio for $SnX_4 \cdot 2L$ adducts, and in a 1:2 Sn/L ratio for $SnX_4 \cdot L{-}L$ adducts. Dibromomethane or nitromethane were used as solvents for the chloride adducts and CH_2Cl_2 for the bromides.

TABLE I. Analytical Results.

Adduct	Sn % calc	found	X % calc	found	C % calc	found	H % calc	found	Y % calc	found
$SnCl_4 \cdot 2Me_2O$	33.66	33.80	40.21	40.10	13.62	13.33	3.43	3.54	9.07	9.11[a]
$SnCl_4 \cdot 2Et_2O$			34.69	34.96	23.51	23.34	4.93	4.93		
$SnCl_4 \cdot 2THF$	29.32	29.50	35.04	34.94	23.74	23.70	3.98	4.11	7.90	8.00[a]
$SnCl_4 \cdot DME$			40.45	40.06	13.70	13.77	2.87	3.22		
$SnCl_4 \cdot 2Me_2S$	30.84	30.59	36.85	36.78	12.48	12.63	3.14	3.26	16.66	16.66[b]
$SnCl_4 \cdot 2Et_2S$			32.46	31.95	21.99	21.65	4.61	4.49		
t-$SnCl_4 \cdot 2THT$	27.17	27.32	32.46	32.25	21.99	22.03	3.69	3.54	14.68	14.56[b]
c-$SnCl_4 \cdot 2THT$	27.17	27.36	32.46	32.33	21.99	22.10	3.69	3.77	14.68	14.69[b]
$SnCl_4 \cdot 2Me_2Se$	24.80	24.53	29.63	29.75	10.04	10.20	2.53	2.61	32.99	32.80[c]
$SnCl_4 \cdot 2Me_2CO$			37.65	37.61	19.13	18.86	3.22	3.32		
$SnCl_4 \cdot 2MeCN$			41.39	41.16	14.02	13.78	1.76	1.93		
$SnCl_4 \cdot 2Me_3CCN$			33.23	33.19	28.14	28.04	4.25	4.41		
$SnCl_4 \cdot 2HMPA$			22.91	23.00	23.29	23.40	5.86	6.03		
$SnCl_4 \cdot 2TMPA$			26.23	26.31	13.33	13.14	3.36	3.33		
$SnBr_4 \cdot 2Me_2S$			56.81	57.09	8.53	8.44	2.15	2.08	11.40	11.19[b]
$SnBr_4 \cdot 2Et_2S$					15.53	15.57	3.26	3.44		
$SnBr_4 \cdot 2Me_2Se$			48.69	48.81	7.32	7.35	1.84	1.88	24.06	24.28[c]
$SnBr_4 \cdot 2HMPA$			40.12	40.04	18.10	18.37	4.55	4.70		
$SnBr_4 \cdot 2TMPA$			44.48	44.73	10.03	10.15	2.52	2.51		

[a]Y = oxygen. [b]Sulfur. [c]Selenium.

Spectral Measurements

IR spectra were recorded with a Perkin–Elmer 577 grating spectrometer, purged with nitrogen. The solid adducts were prepared as Nujol mulls and placed between CsBr or polyethylene windows. The adduct solutions were injected in sealed CsI cells. The spectra were recorded between 600 and 200 cm^{-1}, and calibrated with the 381.4 cm^{-1} band of indene.

Raman spectra were recorded between 600 and 50 cm^{-1} on a 1403 Spex spectrometer using an argon (514 or 488 nm) or a krypton (647 nm) laser. The solid or solution adducts were contained in a capillary tube. Low temperature measurements were made using a Harvey–Miller cell. The 218 cm^{-1} band of CCl_4 was used for calibration.

Abbreviations

Tetrahydrofuran = THF, 1,2-dimethoxyethane = DME, tetrahydrothiophene = THT, hexamethylphosphoramide = HMPA, trimethylphosphate = TMPA.

Results

The *trans*-$SnX_4 \cdot 2L$ isomer, belonging to D_{4h} group symmetry (if L is assumed to be a point mass), has the following vibrational representation:

$$\Gamma_V = 2A_{1g} + B_{1g} + B_{2g} + E_g \quad \text{(R active only)}$$
$$2A_{2u} + 3E_u \quad \text{(IR active only)}$$
$$B_{2u} \quad \text{(inactive)}$$

The three A_{1g}, B_{1g} and E_u modes represent Sn–X stretches, and the two A_{1g} and A_{2u} are Sn–L stretching vibrations. Since bending modes are more difficult to assign, they will not be treated here. The *cis*-$SnX_4 \cdot 2L$ isomer, classified under C_{2v} symmetry, has the following representation:

$$\Gamma_V = 6A_1 + 3B_1 + 4B_2 \quad \text{(IR and R active)}$$
$$2A_2 \quad \text{(R active only)}$$

where the $2A_1 + B_1 + B_2$ modes correspond to Sn–X stretches, and $A_1 + B_2$ to Sn–L stretching vibrations.

As the exclusion rule for IR and R transitions only holds for the centrosymmetrical *trans* isomer, one should be able to distinguish between *cis* and *trans* isomers in comparing their IR and R spectra. In solution, symmetrical modes may be differentiated from unsymmetrical ones, since their Raman bands arise from diffused light having the same polarization as the incident radiation.

The vibrational results are reported in Tables II and III.

Adducts with Nitriles and Acetone

$SnCl_4 \cdot 2MeCN$

Our IR and Raman spectra (Figure 1) show, in the Sn–Cl stretching region (250–380 cm^{-1}), four bands common to both spectra. This suggests a *cis* geometry and we assigned these bands as follows: the band at 367 (IR) and 361 (R) cm^{-1} to the $\nu_7(B_1)$ mode; at 345 (IR) and 346 (R) cm^{-1} to the $\nu_8(B_2)$ mode; at

TABLE II. Sn–Cl Infrared and Raman Vibrational Frequencies (cm^{-1}) for $SnCl_4 \cdot 2L$ and $SnCl_4 \cdot L–L$ Solid Adducts and in Solution.[a,b]

Adduct		*Cis*								*Trans*		
		$\nu_7(B_1)$ IR	R	$\nu_8(B_2)$ IR	R	$\nu_1(A_1)$ IR	R[c]	$\nu_2(A_1)$ IR	R[c]	$\nu_3(E_u)$ IR	$\nu_1(A_{1g})$ R[c]	$\nu_4(B_{1g})$ R
$SnCl_4 \cdot 2MeCN$	*cis*	367 s	361 (8)	345 vs	346(21)	338 vs	333 (100)	305 s	299 (16)			
	in CH_2Br_2	363 vs	–	341 vs	–	–	339 (100)	309 s	309 (21)			
$SnCl_4 \cdot 2Me_3CCN$	*cis*	364 vs	358 (15)	342 vs	–	338 vs	337 (100)	305 s	302 (25)			
	in CH_2Br_2	366 vs	362 (22)	345 vs	346 (sh)	–	339 (100)	310 m	306 (22)			
$SnCl_4 \cdot 2Me_2CO$	*cis*	362 vs	–	–	–	332 vs	333 (100)	306 vs	304 (21)			
	in CH_2Br_2	360 vs	–	–	–	336 vs	336 (100)	305 s	304 (31)			
$SnCl_4 \cdot 2THT$	*cis*	–	–	–	–	325 vs	320 (75)	288 s	282 (100)			
	trans									322 vs	292 (100)	252 (22)
	in $MeNO_2$		–		–		325 (15)		283 (52)		296 (100)	255 (24)
$SnCl_4 \cdot 2THF$	*trans*									344 vs	313 (100)	255 (23)
	in CH_2Br_2		–		–		333 (40)		292 (14)		316 (100)	256 (10)
$SnCl_4 \cdot 2Me_2O$	*cis*	357 vs	359 (5)	–	–	338 vs	336 (100)	298 s	299 (40)			
	in CH_2Br_2		358 (7)		–		338 (50)		302 (20)		322 (100)	260 (10)
$SnCl_4 \cdot 2Me_2S$	*trans*									327 vs	305 (100)	258 (20)
										317 vs	293 (60)	252 (17)
										305 s		
	in CH_2Br_2		–		–		328 (40)		282 (60)		302 (100)	255 (6)
$SnCl_4 \cdot 2Me_2Se$	*trans*									310 vs	281 (100)	239 (10)
	in CH_2Br_2		–		–		320 (15)		267 (40)		281 (100)	244 (7)
$SnCl_4 \cdot 2Et_2O$	*trans*									350 vs	321 (100)	264 (20)
												257 (10)
$SnCl_4 \cdot 2Et_2S$	*trans*									320 vs	292 (100)	251 (14)
	in CH_2Br_2		–		–		328 (22)		278 (25)		296 (100)	254 (7)
$SnCl_4 \cdot DME$	*cis*	360 vs	358 (10)	–	–	340 vs	338 (100)	293 s	291 (45)			
	in $MeNO_2$	360 vs	–		–	342 vs	340 (100)	305 s	295 (30)			
$SnCl_4 \cdot 2HMPA$	*trans*									331 vs	308 (100)	244 (15)
	in CH_2Br_2		–		–		344 (45)		320 (45)		307 (100)	243 (12)
$SnCl_4 \cdot 2TMPA$	*cis*	–	–	335 vs	–	325 vs	327 (100)	295 s	292 (15)			
	in CH_2Br_2		–		–		328 (100)		292 (15)		319 (58)	254 (5)

[a]Abbreviations for IR band intensities: vs = very strong, s = strong, m = medium, sh = shoulder. [b]Raman band intensities are given as percentages of the main peak.
[c]All symmetrical vibrations have Raman polarized bands in solution.

TABLE III. Sn–Br Infrared and Raman Vibrational Frequencies (cm^{-1}) for $SnBr_4 \cdot 2L$ and $SnBr_4 \cdot L–L$ Solid Adducts and in Solution.

Adduct		*Cis*		*Trans*		
		$\nu_1(A_1)$ R[a]	$\nu_2(A_1)$ R[a]	$\nu_3(E_u)$ IR	$\nu_1(A_{1g})$ R[a]	$\nu_4(B_{1g})$ R
$SnBr_4 \cdot 2THT$	*trans*			230 s	181 (100)	152 (27)
						149 (25)
	in CH_2Cl_2	222 (30)	178 (sh)		184 (100)	151 (8)
$SnBr_4 \cdot 2THF$	*trans*			248 s	202 (100)	159 (20)
	in CH_2Cl_2	226 (46)	215 (90)		203 (100)	161 (6)
$SnBr_4 \cdot 2Me_2S$	*trans*			233 vs	206 (47)	155 (26)
				215 s	190 (100)	150 (26)
	in CH_2Cl_2	214 (21)	200 (sh)		188 (100)	153 (8)
$SnBr_4 \cdot 2Me_2Se$	*trans*			230 vs	175 (100)	151 (7)
	in CH_2Cl_2				179 (100)	151 (8)
$SnBr_4 \cdot 2Et_2S$	*trans*			240 vs	184 (100)	155 (9)
						149 (8)
	in CH_2Cl_2	220 (25)	202 (40)		187 (100)	152 (7)
$SnBr_4 \cdot DME$	in CH_2Cl_2	220 (43)	194 (100)			
$SnBr_4 \cdot 2HMPA$	*trans*			240 vs	187 (100)	145 (20)
	in CH_2Cl_2	209 (38)	177 (40)		187 (100)	146 (17)
$SnBr_4 \cdot 2TMPA$	*cis*	209 (73)	186 (100)			
	in CH_2Cl_2	214 (75)	188 (100)			

[a]All symmetrical vibrations have Raman polarized bands in solution.

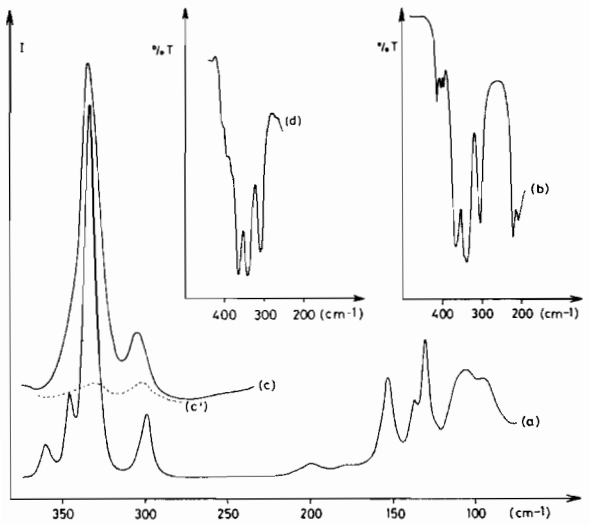

Figure 1. Raman (a) and infrared (b) spectra of the *cis*-$SnCl_4 \cdot 2MeCN$ solid adduct; Raman (c, c') and infrared (d) spectra in CH_2Br_2.

338 (IR) and 333 (R) cm^{-1} to the $\nu_1(A_1)$ mode and at 305 IR) and 299 (R) cm^{-1} to the $\nu_2(A_1)$ mode. The A_1 modes are assigned on the basis of the R polarization solution spectra discussed below; the 367 (IR) and 361 (R) cm^{-1} band is labelled ν_7 (the first six subscripts correspond to A_1 modes), as it appears at the highest energy. The assignment of this band to the B_1 mode is based on the predictions obtained by a normal coordinate analysis on a $SnX_4 \cdot 2L$ model where the Sn–L and Sn–X force constants were varied arbitrarily [2]. The 345 (IR) and 346 (R) cm^{-1} band is then assigned to the $\nu_8(B_2)$ mode. The weak IR bands around 400 cm^{-1} are due to ligand deformation modes as demonstrated by ligand deuteration [3]. Our results complete the assignment of earlier results based on a *cis* configuration [3, 4].

The IR and R spectra in CH_2Br_2 (Figure 1) show the following bands: at 363 (IR) cm^{-1} the $\nu_7(B_1)$ mode, at 341 (IR) cm^{-1} the $\nu_8(B_2)$ mode, at 339 (R) cm^{-1} the $\nu_1(A_1)$ mode and at 309(IR, R) cm^{-1} the $\nu_2(A_1)$ mode. The 339 and 309 cm^{-1} Raman bands show a strong polarization effect, as expected for symmetrical modes. The $\nu_7(B_1)$ and $\nu_8(B_2)$ modes, which are weak in the solid Raman spectrum, are not observed in the Raman solution spectrum due to their low activity. The $\nu_8(B_2)$ and $\nu_1(A_1)$ bands are accidentally superposed at 341 cm^{-1} in the IR spectrum. Contrary to what has been observed in benzene

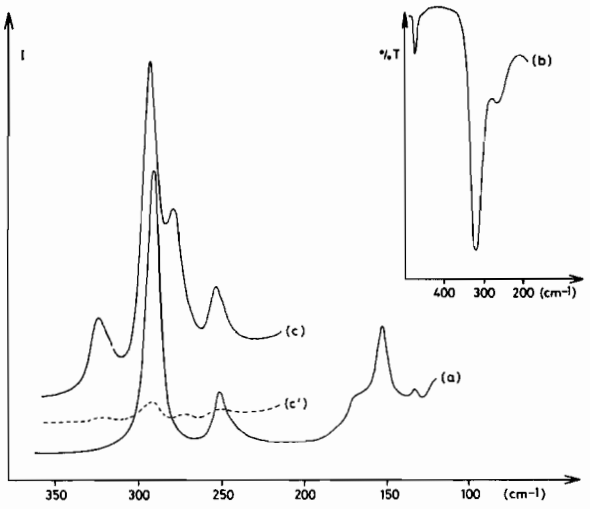

Figure 2. Raman (a) and infrared (b) spectra of the *trans*-$SnCl_4 \cdot 2THT$ solid adduct, and Raman (c, c') spectra in nitromethane.

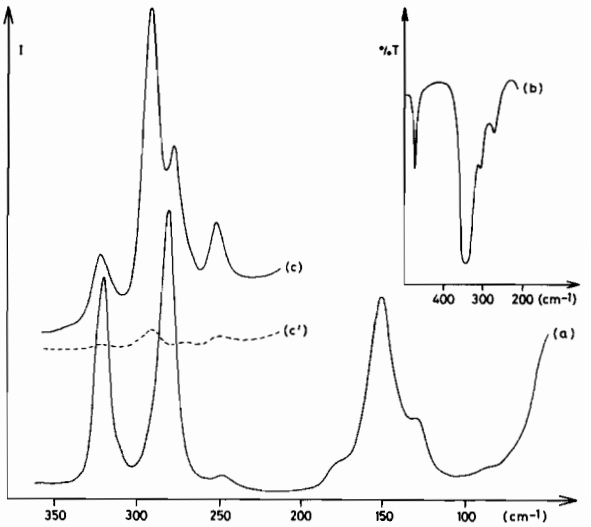

Figure 3. Raman (a) and infrared (b) spectra of the *cis*-$SnCl_4 \cdot 2THT$ solid adduct, and Raman (c, c') spectra in nitromethane.

solution [5], this adduct does not seem to undergo any dissociation in CH_2Br_2. We could not prepare a $SnBr_4 \cdot 2MeCN$ adduct; it has been suggested that this is only stable at low temperature [6]; it was even claimed that a $SnBr_4 \cdot 3MeCN$ was isolated [7]. Our Raman solution spectra only show the characteristic bands of uncomplexed $SnBr_4$.

$SnCl_4 \cdot 2Me_2CO$

Both IR and R spectra of the solid confirm a *cis* geometry. Ligand bending modes appear at 558 and 428 cm^{-1}. In solution, the IR and R spectra only show the presence of the *cis* adduct. The coordinated ligand bending modes appear at 558 and 422 cm^{-1}, while these modes appear at 532 and 391 cm^{-1} for the free ligand. The band appearing at 306 (IR) and 304 (R) cm^{-1} is due to the $\nu_2(A_1)$ mode, and not to a partial hydrolysis of the complex [7, 9].

A $SnBr_4 \cdot 2Me_2CO$ adduct could not be synthesized. The R solution spectra show the free $SnBr_4$ bands, and two weak bands at 212 and 196 cm^{-1}, corresponding to some complex formation.

Adducts with Dialkylchalcogens

$SnCl_4 \cdot 2THT$

A *trans* geometry has been proposed on the basis of X-ray structure analysis [10] and of the IR [8, 11] and Raman [9] spectra. We have synthesized two adducts of this type, the first one in CH_2Cl_2, and the second in n-pentane.

For the first adduct, the IR solid spectrum (Figure 2) shows the characteristic bands of a *trans* isomer: the 322 cm^{-1} band is assigned to the $\nu_3(E_u)$ mode and the 265 cm^{-1} band to the $\nu_5(Sn{-}S)$ (A_{2u}) mode. This *trans* geometry is confirmed by the Raman spectrum (Figure 2), where the 292 and 252 bands are assigned to the $\nu_1(A_{1g})$ and $\nu_4(B_{1g})$ modes respectively. Bands at 522 and 475 (IR) cm^{-1} are due to ligand modes.

For the second adduct the observed frequencies in the Sn–Cl stretching region are common in the IR and R spectra (Figure 3), therefore the assignment is based on a *cis* geometry. The band at 325 (IR) and 320 (R) cm^{-1} is assigned to the $\nu_1(A_1)$ mode, and at 288 (IR) and 282 (R) cm^{-1} to the $\nu_2(A_1)$ mode. Another band appears at 255 (IR) and 249 (R) cm^{-1}, and is probably due to the $\nu_3(Sn{-}S)$ (A_1) mode. The B_1 and B_2 modes are not observed in either the Raman spectrum, probably because of their low activity, nor in the IR spectrum, where the 325 cm^{-1} band is broad enough to contain other modes. Bands at 522 and 473 (IR) cm^{-1} are due to ligand modes.

The Raman solution spectra (Figures 2 and 3) in nitromethane show the *cis* bands at 325 and 283 cm^{-1}, as well as the *trans* ones at 296 and 255 cm^{-1}. The bands at 325, 283 and 296 cm^{-1} are polarized and correspond to symmetrical modes. Another band at 255 cm^{-1} is also polarized, and seems to be due to the superposition of the *trans* $\nu_4(B_{1g})$ mode with the *cis* $\nu_3(Sn{-}S)$ (A_1) mode. This band cannot be due to the *trans* $\nu_2(Sn{-}S)$ (A_{1g}) mode, which lies at lower frequency; in *trans*-$SnCl_4 \cdot 2py$, Ohkaku and Nakamoto [11] have assigned a band at 157 cm^{-1} to the $\nu_2(Sn{-}N)$ (A_{1g}) mode. The IR solution spectrum is of less interest as the resolution is insufficient to differentiate the *cis* A_1, B_1 and B_2 modes from the *trans* E_u mode.

We have clearly established that a *cis–trans* equilibrium is present in solution. The choice of a weakly polar solvent (n-pentane) or a polar one (CH_2Cl_2) determines which isomer will precipitate. In using a solvent of intermediate polarity (n-pentane/CH_2Cl_2

1:1), a mixture of *cis* and *trans* isomers cristallizes. The existence of a *cis–trans* equilibrium explains the high dipole moment (4.2 Debye) obtained by Beattie [10] who argued about a dissociation or a hydrolysis of the *trans* adduct. It also explains the appearance of additional bands to the *trans* ones found in the Raman spectrum, which are not due to a breakdown of the selection rules by a lowering of the symmetry [9], but to the presence of the *cis* adduct.

$SnBr_4 \cdot 2THT$

Our Raman solid spectrum confirms the proposed [11] *trans* geometry, with the bands at 181 and 152, 149 cm^{-1}*, assigned to the $\nu_1(A_{1g})$ and $\nu_4(B_{1g})$ modes respectively. The Raman solution spectra also show a *cis–trans* equilibrium which explains the high dipole moment value (8 Debye) reported [12], which falsely led to the assignment of the *cis* geometry in solution.

$SnCl_4 \cdot 2Me_2O$

As we reported previously [13], the IR and R solid spectra suggest a *cis* geometry, and the Raman solution spectrum shows a *cis–trans* equilibrium. A $SnBr_4 \cdot 2Me_2O$ adduct could not be synthesized. The Raman solution spectra show the bands of uncomplexed $SnBr_4$, and the presence of a weak band at 209 cm^{-1} corresponding to a small amount of complex formation.

$SnCl_4 \cdot 2Me_2S$

The IR and R solid spectra strongly resemble those of a *trans* adduct, but with a systematic splitting of the E_u (327, 317, 305 cm^{-1}), A_{1g} (305, 293 cm^{-1}) and B_{1g} (258, 262 cm^{-1}) modes. The single IR band at 266 cm^{-1} can be assigned to the ν_5(Sn–S) (A_{2u}) mode. The Raman solution spectra show a *cis–trans* equilibrium with the *cis* polarized bands at 328 and 282 cm^{-1}, a single *trans* polarized band at 302 cm^{-1} and a single *trans* depolarized band at 255 cm^{-1}. The splitting of the IR and R bands for the solid adduct cannot be explained by a symmetry lowering of one $SnCl_4 \cdot 2Me_2S$ unit. The presence of two different *trans*-$SnCl_4 \cdot 2Mc_2S$ adducts in the unit cell could explain this splitting.

$SnBr_4 \cdot 2Me_2S$

As with the tetrachloride adduct, the Raman solid spectrum shows a splitting of the A_{1g} and B_{1g} modes which also disappears in the Raman solution spectra where a *cis–trans* equilibrium is observed.

$SnCl_4 \cdot 2Me_2Se$

We have reported previously [13] a *trans* geometry for the solid adduct. The 210 (IR) cm^{-1} band may be due to the ν_5(Sn–Se) (A_{2u}) mode, while a band at 245 (IR) and 249 (R) cm^{-1} is due to the ligand bending mode. The Raman solution spectra show a *cis–trans* equilibrium.

$SnBr_4 \cdot 2Me_2Se$

The Raman solid spectrum suggests a *trans* geometry. The Raman solution spectra show the presence of the *trans* isomer only. Another polarized band appears at 116 cm^{-1}, and may be assigned to the ν_2(Sn–Se) (A_{1g}) mode; this band is also present in the solid spectrum at 121 cm^{-1}. However, the NMR spectrum [19] taken at –90 °C shows the existence of a *cis–trans* equilibrium, but with little *cis* isomer present ([*trans*]/[*cis*] = 2.33). A Raman solution spectrum run at the same temperature only shows the *trans* isomer. It is a general observation in our systems that the characteristic *cis* Raman bands, $\nu_1(A_1)$ and $\nu_2(A_1)$, are less active than the *trans* $\nu_1(A_{1g})$ one. Consequently, it is difficult to reveal a small amount of the *cis* isomer in equilibrium with the *trans* one by Raman spectroscopy.

$SnCl_4 \cdot 2Et_2O$

The IR and R solid spectra are in agreement with the *trans* geometry, proposed by other workers [8, 9, 14]. The Raman solution spectra show polarized bands additional to the *trans* ones (320, 260 cm^{-1}), appearing at 364, 348 and 337 cm^{-1}. Compared to the $\nu_1(A_1)$ and $\nu_2(A_1)$ vibrations of other *cis* adducts, the 364 and 348 cm^{-1} bands are due to other species. It has been shown [15] that this adduct is partially dissociated in benzene. The additional bands observed may be due to Sn–Cl modes of a pentacoordinate species, or even to the ν_1(Sn–Cl) (A_1) mode of free $SnCl_4$ at 364 cm^{-1}.

A $SnBr_4 \cdot 2Et_2O$ adduct could not be synthesized. The Raman spectra in CH_2Cl_2 or Et_2O only show the characteristic bands of uncomplexed $SnBr_4$; this confirms that this adduct is strongly dissociated [16] in solution.

$SnCl_4 \cdot 2Et_2S$

The IR and R solid spectra are in agreement with the *trans* geometry proposed previously [8]. The IR band at 210 cm^{-1} may be assigned to the ν_5(Sn–S) (A_{2u}) mode, and bands at 390 (IR), 385 (R) and 334 (R) cm^{-1} arise from ligand vibrational modes. A *cis–trans* equilibrium is observed in the Raman solution spectra, contrary to the results of Beattie [9] who only observed the presence of the *trans* isomer.

$SnCl_4 \cdot DME$

A *trans* geometry has been proposed on the basis of the IR [8] and NQR [14, 17] spectra, while Errington and Clark [18] deduced a *cis* geometry from their IR data. Our IR and R solid spectra show a *cis* geometry for this adduct, and only this isomer is

*One of these two bands could not be assigned.

found in the Raman solution spectra. NMR spectroscopy confirms the absence of a *trans* adduct [19].

$SnBr_4$·DME

On the basis of the NQR spectrum, a *trans* geometry was proposed [20]. Our Raman solid spectrum shows a large number of bands which cannot be easily identified. One possibility is a complex structure of *trans* bridged units. The Raman solution spectra are much simpler and show the two characteristic polarized bands of a *cis* isomer. A depolarized band appears at 244 cm^{-1} and may be assigned to the ν_9(Sn–O) (B_2) mode. The NMR spectrum [19] confirms the presence of the *cis* adduct only.

Adducts Formed with Phosphorylated Ligands

$SnCl_4$·2HMPA

The IR and Raman solid spectra suggest a *trans* geometry. Bands at 480 (IR), 395 (IR) and 380 (R), 356 (R), and 310 (IR) cm^{-1} are due to ligand modes. The Raman solution spectra indicate the presence of a *cis–trans* equilibrium. A polarized band appearing at 229 cm^{-1} may be assigned to the ν_3(Sn–O) (A_1) mode.

$SnBr_4$·2HMPA

Contrary to NQR results [20], where a *cis* geometry was proposed, our Raman solid spectrum suggests a *trans* configuration. The Raman spectra in CH_2Cl_2 reveal a *cis–trans* equilibrium. We also recorded Raman spectra in $CHCl_3$ and CH_2Cl_2/$MeNO_2$ (3:1) (Figure 4); the *cis* and *trans* bands have been deconvoluted manually, and the ratio of the *trans* band to any *cis* band clearly shows that the *trans* isomer is favoured by lowering the solvent polarity.

$SnBr_4$·2TMPA

A *cis* geometry is demonstrated for the solid adduct by our Raman spectrum. Only the *cis* isomer is found in the Raman solution spectra. However, the NMR spectrum [19] indicates the existence of a *cis–trans* equilibrium, but with little *trans* isomer formation.

Discussion

Some general remarks can be made about the vibrational spectra of SnX_4·2L adducts. The Raman solid spectra for a *trans* isomer generally show an intense band around 300 cm^{-1} for chloride adducts, and 200 cm^{-1} for bromide ones, corresponding to the $\nu_1(A_{1g})$ mode. A second much weaker band appears around 250 or 150 cm^{-1} for the chloride or the bromide adduct respectively, corresponding to the $\nu_4(B_{1g})$ mode. For the *cis* adduct, two bands are

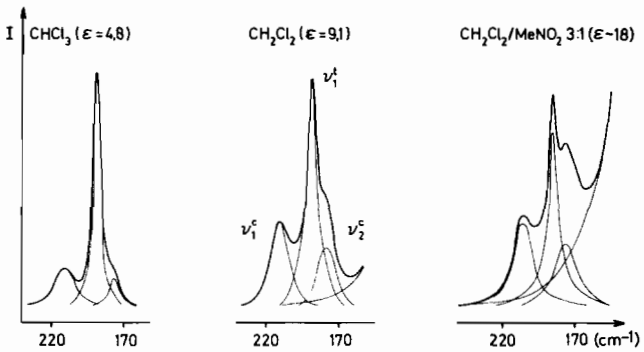

Figure 4. Raman intensity ratios for the *cis*- $\nu_1^c(A_1)$, $\nu_2^c(A_1)$ and *trans*- $\nu_1^t(A_{1g})$ modes of $SnBr_4$·2HMPA for different solvent polarities:

	$CHCl_3$	CH_2Cl_2	CH_2Cl_2/$MeNO_2$ 3:1
$I(\nu_1^t)/I(\nu_1^c)$	2.8	1.8	1.4
$I(\nu_1^t)/I(\nu_2^c)$	5.9	2.8	1.8

observed in the Raman solid spectra, corresponding to the A_1 modes. Their intensities are more nearly equal than the *trans* bands discussed above. The B_1 and B_2 modes are very weak or often not observed. The IR solid spectra are often confusing, since the $\nu_3(E_u)$ mode for a *trans* compound shows a large band which may split, and a spectrum resembling one for a *cis* isomer may be obtained. When a *cis–trans* equilibrium is present in solution, IR spectra only show a broad band covering all modes. Raman spectroscopy alone allows the discrimination between both isomers, and it is often observed that the $\nu_1(A_{1g})$ *trans* mode lies between the two *cis* A_1 modes. Special attention must be paid since intensity ratios may vary between solution and solid spectra.

The frequency shift of the $\nu_1(A_{1g})$ mode of a *trans* adduct accompanying the halogen substitution, also confirms our assignment by the constancy of the ratio ν_1(Sn–Br) (A_{1g})/ν_1(Sn–Cl)(A_{1g}) (Table III); this ratio is close to $(\mu_{Br}/\mu_{Cl})^{1/2} = 0.66$, as expected in the harmonic potential approximation.

It is a common fact [11] to correlate the Sn–X stretching frequency for different adducts to the strength of the Sn–L bond: the stronger the Sn–L bond, the lower the Sn–X frequency observed. This hypothesis is mostly reasonable for a homologous series like the dialkylchalcogen ligands, where it has been assumed [21] that the same ligand orbital is involved in bond formation. Referring to Table II, the following frequency sequence for the ν_1(Sn–Cl) (A_{1g}) mode of *trans* adducts may be written:

$$Me_2O \sim Et_2O \sim THF > Me_2S \sim Et_2S \sim$$

$$THT > Me_2Se.$$

This suggests that the Sn–L strength increases in going from oxygen to selenium donors. A similar sequence is obtained for the ν_1(Sn–Br) (A_{1g}) mode. One could write a comparable sequence for the ν_1-

TABLE IV. ν(Sn–Br)/ν(Sn–Cl) Frequency Ratio for the $\nu_1(A_{1g})$ Mode of *trans*-$SnX_4 \cdot 2L$ Adducts.

	THF	THT	Me_2S	Et_2S	Me_2Se	HMPA
$\frac{\nu(Sn-Br)}{\nu(Sn-Cl)}$	0.64	0.62	0.62	0.63	0.64	0.61

(A_1) and $\nu_2(A_1)$ modes of *cis* adducts. In this case however, there might be a coupling between these modes and other modes of the same symmetry, as for example ν_3(Sn–L) (A_1). For the dialkylchalcogen ligands, one observes that the $\nu_1(A_1)$ and $\nu_2(A_1)$ Sn–Cl frequencies also decrease from oxygen to selenium donors. Whereas with phosphorylated ligands, the *trans* $\nu_1(A_{1g})$ mode appears at 319 cm^{-1} for $SnCl_4 \cdot$-2TMPA, and at 307 cm^{-1} for $SnCl_4 \cdot 2$HMPA. The order is inverted for the $\nu_1(A_1)$ and $\nu_2(A_1)$ modes appearing at 328 and 292 cm^{-1} for $SnCl_4 \cdot 2$TMPA, and at 344 and 320 cm^{-1} for $SnCl_4 \cdot 2$HMPA.

One may estimate from the Sn–X stretching frequencies in *trans*-$SnX_4 \cdot 2L$ adducts the Sn–X force constant f_r, the interaction force constants between two adjacent Sn–X bonds f_{rr}, and between two opposite Sn–X bonds f'_{rr}. We shall assume in these calculations that coupling between these Sn–X stretching modes with other modes of the same symmetry is negligible. In this estimation, we neglect the coupling between the Sn–X stretching modes with bending modes and Sn–L stretching of the same symmetry, as the former modes lie at much higher energies.

The following F–G terms of the Wilson matrix, calculated in a General Valence Force Field GVFF, are obtained for the Sn–X stretching modes [2]:

$$A_{1g} : F_{11} = f_r + 2f_{rr} + f'_{rr} \quad G_{11} = \mu_X$$

$$B_{1g} : F_{44} = f_r - 2f_{rr} + f'_{rr} \quad G_{44} = \mu_X$$

$$E_u : F_{33} = f_r - f'_{rr} \quad G_{33} = \mu_X + 2\mu_{Sn}$$

These F–G blocks may be resolved by the relation $G_{ii}F_{ii} - E\lambda_i = 0$, where λ_i is the eigenvalue defined by

$$\lambda_i = 0.58915 \left(\frac{\nu_i}{1000}\right)^2 = G_{ii}F_{ii},$$

where the masses are expressed in atomic weights, and force constants in mdyn/Å. Knowing the ν_i frequency of these modes, one may calculate the force constants with:

$$f_r = \frac{1}{4}[\lambda_1/\mu_X + \lambda_4/\mu_X + 2\lambda_3/(\mu_X + 2\mu_{Sn})]$$

$$f'_{rr} = f_r - \lambda_3/(\mu_X + 2\mu_{Sn})$$

$$f_{rr} = \frac{1}{4}(\lambda_1/\mu_X - \lambda_4/\mu_X)$$

The calculated force constants are reported in Table V for the homologous series with the dialkylchalcogen and the phosphorylated ligands. As the ν_3(Sn– Cl) (E_u) mode could not be clearly assigned for the *trans* $SnCl_4$ adducts with Me_2O, Me_2S and TMPA, we have calculated the f_r force constants using mean values for f_{rr} and f'_{rr} for the oxygen donors (f_{rr} = 0.18, f'_{rr} = 0.08) and for the sulfur donors (f_{rr} = 0.11, f'_{rr} = 0.10). The following equation was then used:

$$f_r = \frac{0.58915}{\mu_X}\left(\frac{\nu_1(A_{1g})}{1000}\right)^2 - (2f_{rr} + f'_{rr})$$

The force constant sequences obtained in both cases correspond to those observed earlier for the ν_1-(Sn–X) (A_{1g}) stretching frequencies. The discrimination between the calculated force constants as a function of the ligand L is greater for the chloride than for the bromide adducts. This may be due to a more pronounced coupling between both ν_1(Sn–Br) (A_{1g}) and ν_2(Sn–L) (A_{1g}) modes.

TABLE V. Sn–X GVFF Force Constants (mdyn/Å) Calculated for *trans*-$SnX_4 \cdot 2L$ Solid Adducts.

	Me_2O[a]	Et_2O	THF	Me_2S[a]	THT	Et_2S	Me_2Se	TMPA[a]	HMPA
$SnCl_4 \cdot 2L$									
f_r	1.71	1.68	1.63	1.47	1.46	1.44	1.34	1.69	1.52
f_{rr}	0.18	0.19	0.17	0.11	0.11	0.11	0.11	0.18	0.18
f'_{rr}	0.08	0.08	0.08	0.10	0.10	0.10	0.08	0.08	0.09
$SnBr_4 \cdot 2L$									
f_r			1.39	1.30	1.18	1.23	1.16		1.24
f_{rr}			0.18	0.13	0.12	0.14	0.10		0.16
f'_{rr}			0.15	0.10	0.12	0.08	0.10		0.08

[a] f_r is calculated from the $\nu_1(A_{1g})$ mode, and from mean values adopted for f_{rr} and f'_{rr}.

Our Raman solution spectra for the majority of these adducts revealed the existence of a *cis–trans* equilibrium. The conclusion [10] that weakly steric hindered ligands favour a *cis* configuration should be considered with care; these assumptions were based on solid spectral results and we have shown with $SnCl_4 \cdot 2THT$ that either a *cis* or a *trans* adduct can be synthesized by changing the solvent polarity. Additionally, weakly hindered ligands like Me_2O give rise to *cis–trans* equilibrium as well as more sterically hindered ligands like Me_2Se. The steric hindrance can be only one factor influencing the *cis–trans* isomerization.

Our vibrational results encouraged us to quantify the parameters which govern these equilibria. In a following paper [19] we shall present a study of the influence of the solvent polarity, the halogen nature, the temperature, the ligand donor strength and the sterical hindrance on the *cis–trans* isomerization.

Acknowledgments

We are indepted to Dr. C. W. Schläpfer for fruitful discussions. We acknowledge the generous support of the Fonds National Suisse de la Recherche Scientifique, through grant 2.476-0.75.

References

1 J. M. Dumas and M. Gomel, *Bull. Soc. Chim. France, 10,* 1885 (1974).
2 I. R. Beattie, M. Webster and G. W. Chantry, *J. Chem. Soc.,* 6172 (1964).
3 M. Webster and H. E. Blayden, *J. Chem. Soc. A,* 2443 (1969).
4 M. F. Farona and J. G. Grasselli, *Inorg. Chem., 6,* 1675 (1967).
5 I. R. Beattie, G. P. McQuillan, L. Rule and M. Webster, *J. Chem. Soc.,* 1514 (1963).
6 N. A. Puschin, M. Ristic, I. Parchomenko and J. Ubovic, *Ann., 553,* 278 (1942).
7 R. A. Slavinskaya, I. G. Litvyak, L. V. Levchenko, T. N. Sumarokova and A. B. Karelova, *Zh. Obshch. Khim., 39,* 487 (1969).
8 I. R. Beattie and L. Rule, *J. Chem. Soc.,* 3287 (1964).
9 I. R. Beattie and L. Rule, *J. Chem. Soc.,* 2995 (1965).
10 I. R. Beattie, R. Hulme and L. Rule, *J. Chem. Soc.,* 1581 (1965).
11 N. Ohkaku and K. Nakamoto, *Inorg. Chem., 12,* 2440 (1973).
12 J. Philip, M. A. Mullins and C. Curran, *Inorg. Chem., 7,* 1895 (1968).
13 S. J. Ruzicka and A. E. Merbach, *Helv. Chim. Acta, 58,* 586 (1975).
14 E. A. Kravchenko, Y. K. Maksyutin, E. N. Guryanova and G. K. Semin, *Izv. Akad. Nauk. SSSR, Ser. Khim., 6,* 1271 (1968).
15 A. W. Laubengayer and W. C. Smith, *J. Am. Chem. Soc., 76,* 5985 (1954).
16 H. H. Sisler, E. E. Schilling and W. O. Groves, *J. Am. Chem. Soc., 73,* 426 (1951).
17 Y. K. Maksyutin and E. N. Guryanova, *Chem. Comm.,* 429 (1973).
18 R. J. H. Clark and W. Errington, *Inorg. Chem., 5,* 650 (1966).
19 To be published.
20 V. S. Petrosyan, N. S. Yashina, O. A. Reutov, E. V. Bryuchova and G. K. Semin, *J. Organometal. Chem., 52,* 321 (1973).
21 S. Cradock and R. A. Whiteford, *J. Chem. Soc. Faraday II,* 281 (1972).
22 K. Nakamoto, 'Infrared Spectra of Inorganic and Coordination Compounds', Wiley–Interscience, New York, 1963.